FULL PAPER

Fabrication of Patterned Concave Microstructures by Inkjet Imprinting

*Bin Bao, Jieke Jiang, Fengyu Li, Pengchao Zhang, Shuoran Chen, Qiang Yang, Shutao Wang, Bin Su, Lei Jiang, and Yanlin Song**

Concave microstructures such as microwells and microgrooves are widely utilized in fields such as biochips, microfluidics, and functional devices. Previously, concave microstructure fabrication was mostly based on laser etching or lithography which is either costly or of multisteps. The inkjet etching method is a direct structuring technique, but limited by its inherent transverse ink diffusion that leads to low feature resolution. Nanoimprint lithography can reach submicro and even nano ranges, whereas an elaborate template is needed. Thus, it is still a challenge to realize controllable fabrication of concave microstructures in large areas with high efficiency and resolution. Here, a template-free strategy to fabricate concave microstructures with high resolution by inkjet imprinting is provided. In this method, a sacrificial ink is inkjet-printed onto a precured viscoelastic surface and imprints its shapes to construct concave microstructures. The morphology of the microstructures could be adjusted by controlling the interaction between the two immiscible phases. The microwells/microgrooves could be used to pattern single cells and functional materials such as optical, electronic, and magnetic nanoparticles. These results will open a new pathway to fabricate concave microstructures and broaden their applications in various functional devices.

1. Introduction

Patterned concave microstructures are of significance in many fields such as electronics,[1] optics,[2] and biology,[3] hence various methods have been developed to fabricate these fine structures. As a versatile microstructure fabricating technique, laser etching is extensively utilized to manufacture wells and grooves in the micro and nanometer scales,[4] but it is expensive and inefficient for large area fabrication. Lithography is an effective microstructuring technology, which has been widely used to pattern functional materials with applications ranging from integrated circuits, optoelectronic devices, and microfluidics to microelectromechanical systems.[5] Although conventional lithography works phenomenally well for such numerous microfabricating tasks, it suffers from disadvantages such as multistep, high cost, and heavy pollution. Single-step lithography of micro-optical elements was also demonstrated by applying photoimaging of hybrid glass materials, which represented a significant improvement of traditional lithography.[6]

As an attractive alternative to lithography, inkjet printing is expected to play an increasingly important role for material patterning because of its direct-writing and maskless process, which leads to significant savings in materials usage.[7] So far, inkjet printing has been ubiquitously applied to fabricate functional devices such as high-resolution electrodes,[8] field-effect transistors,[9] solar cells,[10] light-emitting devices,[11] chemical sensors,[12] and bio-printed tissues.[13] Besides depositing functional components on various surfaces, inkjet printing can also serve as an etching technique to fabricate concave microstructures such as microwells and microgrooves. The relief-like microstructures are constructed by site-selectively removing previously deposited materials through the evaporation of the printed solvents, taking advantages of the coffee ring effect.[14] However, the transverse diffusion of the printed ink leads to feature resolutions on the order of dozens to hundreds of micrometers. The etching depth of the microstructures reported so far is only in submicrometer range, because of the limited penetration of the solvent ink. These drawbacks limit the application of the inkjet etching technique. Although nanodents could be fabricated on a polymer–liquid interface by using the second liquid droplet as a template,[15] the randomly generated dents possessed a large size distribution because the size of the emulsion droplet templates is uncontrollable. Hence, it still is a challenge to realize fabrication of concave microstructures with controllable morphology and high resolution in a low cost, highly efficient, and flexible way.

Dr. B. Bao, J. Jiang, Dr. F. Li, Dr. P. Zhang, Dr. S. Chen, Dr. Q. Yang, Prof. Dr. S. Wang, Dr. B. Su, Prof. Dr. L. Jiang, Prof. Dr. Y. Song
Beijing National Laboratory for Molecular Sciences (BNLMS)
Key Laboratory of Green Printing
Key Laboratory of Organic Solids
Institute of Chemistry
Chinese Academy of Sciences
Beijing 100190, P. R. China
E-mail: ylsong@iccas.ac.cn
Dr. B. Bao, J. Jiang, Dr. P. Zhang, Dr. S. Chen, Dr. Q. Yang
School of Chemistry and Chemical Engineering
University of Chinese Academy of Sciences
Beijing 100049, P. R. China
DOI: 10.1002/adfm.201500908

Recently, the nanoimprint lithography (NIL) has been vastly used in micro-/nanofabrication by pressing a model into a thermoplastic polymer film to create vias and trenches.[16] Although the resolution is highly improved, this technique is dependent on elaborately fabricated templates. Combining the advantages of the inkjet etching and NIL techniques, herein we introduce a template-free micofabricating strategy called inkjet imprinting (IIP) to fabricate concave microstructures. Previously, most inkjet printing processes have been carried out on rigid solid substrates such as metals, polymers, and silicon wafers.[17] In this IIP method, viscoelastic surfaces are used as the printing substrates, which show special wettabilities because of the viscoelastic dissipation of spreading liquid on such substrates.[18] Moreover, on these substrates the deposited liquids could induce deformation of the underlying surfaces,[19] which makes them a good candidate material for the fabrication of concave microstructures. The essence of this IIP technique is that immiscible polymer solution ink droplets imprint the shapes of the solute onto precured viscoelastic substrates after solvent evaporation and substrate solidification. Microwells/microgrooves are constructed after the sacrificial polymer solute is rinsed (**Figure 1**a). The morphologies of the microwells/microgrooves could be well adjusted by controlling the interactions between the immiscible ink and the viscoelastic substrates. By adjusting the size of the microwells, single cells could be trapped in the microwells to form single cell arrays, providing a very attractive strategy for single cell level analyses.[20] Furthermore, functional materials such as optical, electronic, and magnetic nanoparticles (NPs) could be patterned in the microgrooves and subsequently transfer-printed to flexible plastics. This novel methodology would open a new avenue for microfabrication. By broadening the combination of the viscoelastic substrates and the immiscible printing inks, the IIP technique could be anticipated to find

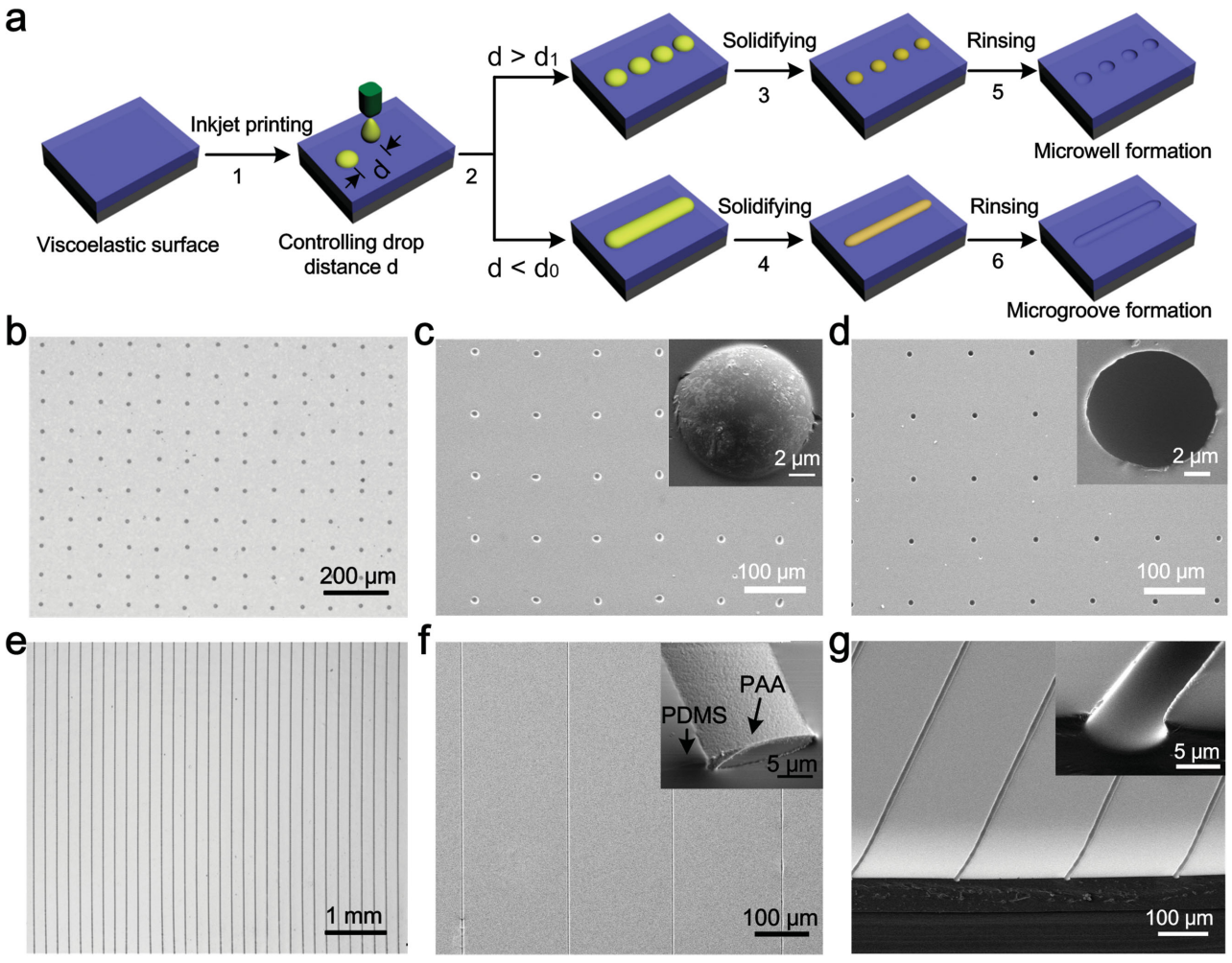

Figure 1. Fabrication of concave microstructures by IIP. a) Schematic illustration of the IIP processes. PAA ink is inkjet-printed onto the precured viscoelastic PDMS surfaces (1). The formation of either microdots or microwires is dependent on the printed ink drop distance *d* (2). After solidification of the ink and the PDMS substrate, microdots and microwires are formed (3 and 4). Finally, concave structures including microwells and microgrooves are constructed on the surfaces by rinsing away the sacrificial PAA ink (5 and 6). b,e) Optical images of the microwell and microgroove arrays. c,f) SEM images of the printed microdots and microwires. Insets in (c) and (f) are amplified images of a single dot and 45° view of a single PAA mirowire, respectively. d,g) SEM images of the microwells and microgrooves after the sacrificial ink is rinsed. Insets in (d) and (g) are amplified images of a single well and groove, respectively.

numerous applications in microfluidics, biochips, functional devices, and so forth.

2. Results and Discussion

2.1. Fabrication and Characterization of Microwells and Microgrooves

Figure 1 demonstrates the large area fabrication of concave microwells and microgrooves by IIP. A schematic illustration of the IIP processes is presented in Figure 1a. Precured polydimethylsiloxane (PDMS) surfaces were selected as printing substrates because they were vastly used in microfluidic chip fabrication due to their straightforward and low fabrication cost,[21] and more importantly, they could change from viscous liquid to viscoelastic state and to solid state with successive heating (will be discussed in details later). Aluminum wafer coated with a rough alumina surface was selected as the supporting layer (Figure S1, Supporting Information), which could keep the spin-coated PDMS precursor tightly thus avoiding outflow of the precursor during substrate handling. Actually, other substrates such as glass, metal, and transparent plastics polyethylene terephthalate (PET) could also be utilized as supporting layers depending on the usage of the fabricated films. In the later experiments alumina surfaces were used unless otherwise noted. The spin-coated PDMS surfaces were extremely smooth after solidification (Figure S2a, Supporting Information). The thickness of the PDMS layer was mainly dependent on the spin-coating conditions, which we used here was about 40 μm (Figure S2b, Supporting Information).

Figure 1b–g demonstrates the structural details and the high uniformity and regularity of the IIP-fabricated microstructures, including 0D microdots and microwells, 1D microwires and microgrooves. Microdot arrays were fabricated by setting the drop distance as 100 μm. For the particular printing condition (substrate heated at 80 °C for 20 min, ink concentration of 16 wt%), single dots with 12.5 ± 0.9 μm in diameter and about 3 μm in height were fabricated. Figure 1c demonstrates that the coffee ring effect was eliminated because of the dewetting of the ink on the viscoelastic PDMS surfaces.[7c] Moreover, the continuous compressing of the surrounding viscoelastic PDMS precursor during the evaporation of the solvent in the ink resulted in printed dots with diameter much smaller than that of the printing nozzle. Microwells with diameter of 9.6 ± 0.6 μm and depth of 1–2 μm were constructed on the surface after the sacrificial inks were removed by water rinsing (Figure S3, Supporting Information). When the distance between the adjacent droplets was reduced down to 20 μm, microgrooves were fabricated, as shown in Figure 1e–g and Figure S4 (Supporting Information). The fabrication could be conducted in large scales and the microgrooves showed great size homogeneity. The length of the microgrooves could be more than a dozen centimeters, limited only by the dimensions of the sizes of the printing substrate. The width and depth of the microgrooves was ≈8.7 μm and 4.4 μm, using 20 min-heated PDMS as substrates and 12 wt% poly acrylic acid (PAA) solution as printing ink. Compared with the diameter of the printing nozzle (25 μm), the width of the microgrooves was much smaller because of the horizontal dewetting and vertical sinking of the ink solution in the viscoelastic PDMS surfaces during its solvent evaporating process. Different from microgrooves made by laser etching or photolithography with square-shaped sectional profiles,[22] the sectional profile of the microgrooves fabricated by IIP was cambered (Figure S4a, Supporting Information). This manifested that the printed PAA ink was tightly encompassed by the viscoelastic PDMS precursor, which could lead to lowest energy for the system.

2.2. Investigation of the Formation Condition of the Concave Microstructures

The viscoelastic state of the PDMS substrates was a key requirement for the formation of concave microstructures, as shown in **Figure 2**. Through quantitative assessment of Fourier transform infrared (FTIR) characterization of the PDMS precursor, the dependence of the precured degree of PDMS surfaces on the precuring time was determined (Figure S5, Supporting Information).[23] With the increase of the precured degree, the PDMS surface changed from viscous liquid to viscoelastic state and finally to solid state (Figure 2c), which led to three typical scenarios of the printed dot formation (Figure 2a,b). With a short precuring time, the precured degree of the PDMS precursor was relatively low. Under this circumstance the surface was viscous liquid-like and the printed ink droplet was without sufficient support, hence sunk underneath the surface (Figure 2a, left panel and Figure S6a, Supporting Information). Whereas the surface became solid-like with elongated precuring time (longer than 30 min at 80 °C), the printed ink droplets could not penetrate the surface. Thus, the surface remained flat after water rinsing, as shown in Figure 2a, right panel and Figure S6c (Supporting Information). With the precured degree ranging from ≈27.2% to ≈84.4%, the PDMS surface became viscoelastic solid-like, in which state it showed peculiar deformation property. As shown by the nanoindentation tests in Figure S7c,d (Supporting Information), an imprint was left on the surfaces after a small external force was exerted onto it and subsequently retreated. The duration of the exerted force was several minutes. On the contrary, the exerted force could not induce deformation on solid surfaces, suggesting that concave structures could not be constructed by printing on these solid surfaces (Figure S7a,b, Supporting Information). These results indicated that the force-induced deformation of the surfaces was a prerequisite for the formation of concave microstructures and concave microwells could only be formed on viscoelastic surfaces with suitable precured degree (Figure 2a, middle panel and Figure S6b, Supporting Information). Direct observation of the ink solution droplet penetration processes further confirmed that microwells were constructed on viscoelastic surfaces, as shown in Figure S8 (Supporting Information).

Besides microwell structures, microgrooves could be fabricated by IIP through the coalescence of individual sacrificial ink drops.[24] As shown in **Figure 3**a, continuous ink lines were obtained by decreasing the ink drop distance down to 20 μm. It was noteworthy that the viscoelastic state of the surface was essential for the formation of continuous ink lines hence the microgrooves. By increasing the precured degree of the

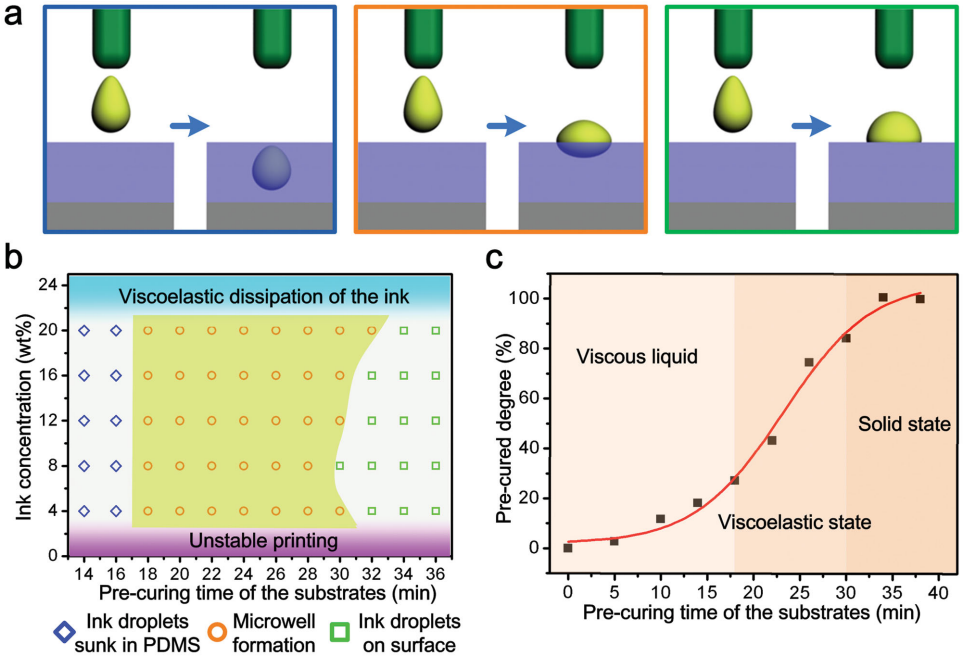

Figure 2. Formation conditions of microwells fabricated by IIP. a) Schematic illustrations of three typical scenarios with printing inks onto viscous liquid surface, viscoelastic surface, and solid surface, respectively. b) The dependence of microwell formation on the precuring time of the PDMS substrates. Within a printable ink concentration range (too low leads to unstable printing because of the low ink viscosity, while too high results in block due to the viscoelastic dissipation of the concentrated ink), concave micowells can only be formed on viscoelastic PDMS substrates with proper heating time that defines the precured degree of the substrates, as shown in c). When heated at 80 °C, the PDMS precursor is cured from viscous liquid to viscoelastic state to solid state successively. The change of precured degree with the heating time is diagrammatically demonstrated in (c).

substrates, drastic changes were observed when the PAA ink was printed. On viscous liquid surface the printed ink droplets coalesced into bigger ones and subsequently sunk underneath the surface (Figure 3b, left panel). Whereas printing on solid PDMS surface resulted in Rayleigh instability of the ink lines because of the isotropic dewetting of the ink on the hydrophobic solid PDMS surfaces (Figure 3b, right panel).[25] Continuous ink lines could only be constructed on viscoelastic substrates, where the imprints of the sacrificial ink lines were kept after solidification of the substrates (Figure 3b, middle panel). The underlying imprints determined the shape of the microgrooves after the sacrificial inks were removed.

2.3. Modulating the Morphology of the Microgrooves

The morphology of the as-fabricated microgrooves was determined by the interaction between the immiscible sacrificial ink and the viscoelastic PDMS substrates, which could be adjusted by controlling printing conditions such as the viscoelasticity of substrates, concentration of ink, and layers of overlap printing (Figure 3c–f). As shown in Figure 3c, increasing the precuring time of the substrates would increase the viscoelasticity of substrates hence increase the spreading widths of inks, which led to wider and shallower microgrooves. The width of the microgrooves increased from 8.7 μm to 14.4 μm with the increasing of the precuring time from 18 min to 26 min at 80 °C. At the same time the depth of the microgrooves decreased from 6.2 μm down to 4.5 μm. When the precured degree of the PDMS surfaces was fixed, the structure parameters of the microgrooves were depended on the concentration of the sacrificial inks (Figure 3d). The width and depth of the microgrooves first increased then decreased with the increase of the PAA ink concentration. The maximum width and depth of the microgrooves appeared at concentration of 16 wt%. This was mainly because the volume of the inkjet-printed droplets decreased at higher concentration since the viscous dissipation of the concentrated PAA inks.[26] As the adjustable range of the microgroove morphology was limited by only changing precured degree of substrates or PAA ink concentrations, overlap printing was carried out to achieve a wider adjusting scope.[27] As shown in Figure 3e,f and Figure S9 (Supporting Information), one to ten layers of PAA ink were overlap-printed on the same spots, hence microgrooves with different cross-sectional views were obtained. The width of the microgrooves increased from 9.4 μm to 36.8 μm and the depth increased from 4.9 μm to 16.9 μm with the increase of the overlap printing numbers. It was believed that the adjustable range could be further extended by cooperatively changing the abovementioned printing conditions, simultaneously.

2.4. Fabrication of 2D Microgroove Networks

2D microgroove networks could also be fabricated by printing in different directions, as demonstrated in Figure S10 (Supporting Information). Optical images of two typical microgroove networks with crossing angles of 90° and 45° are shown in Figure S10a, c (Supporting Information), which demonstrate

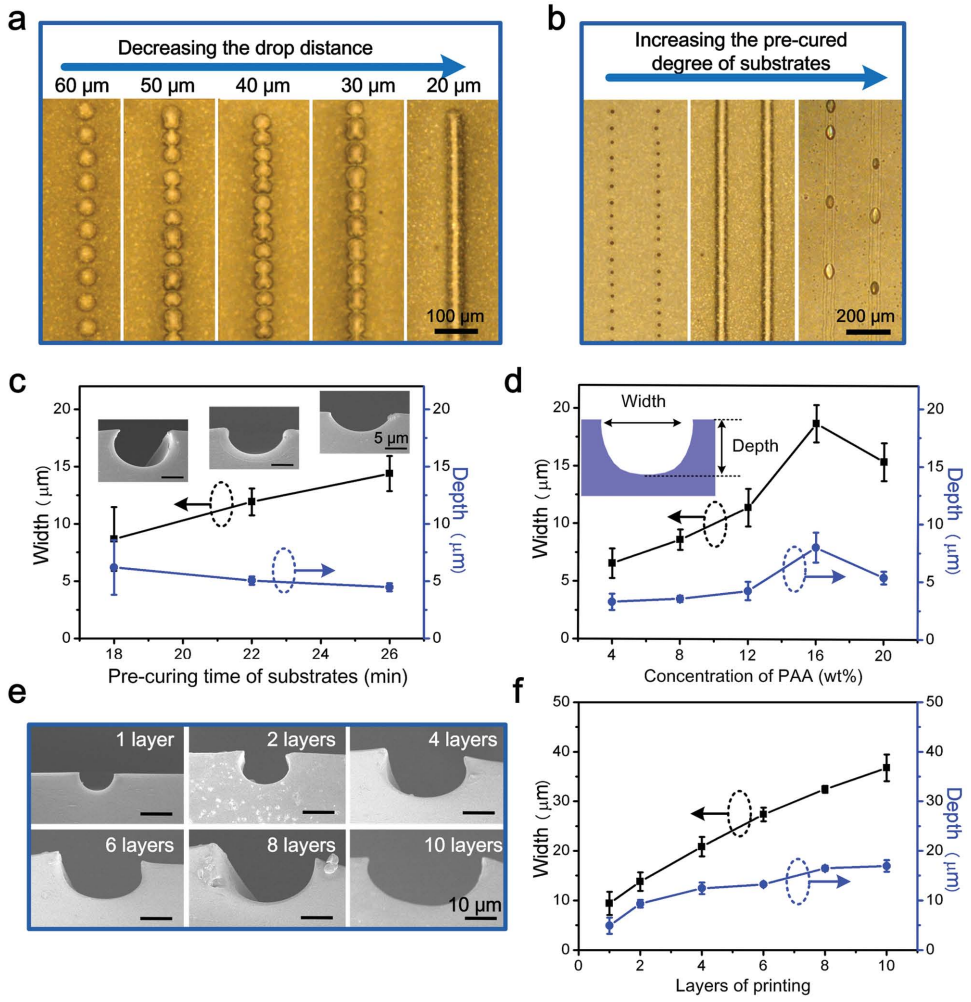

Figure 3. Fabrication of microgrooves with controllable morphologies by IIP. a) Continuous ink lines can be obtained on the viscoelastic PDMS surfaces by decreasing the ink drop distance. From the left to the right panel the drop distance decreases from 60 to 20 μm. Continuous lines can be formed when the drop distance is reduced to 20 μm. b) Viscoelastic surface is essential for continuous line formation. On viscous liquid surface the printed ink droplets coalesce into bigger ones and subsequently sink underneath the surface (left panel), whereas printing on solid PDMS surface results in Rayleigh instability of the ink lines (right panel). Continuous ink lines can only be formed on viscoelastic substrates, where the imprints of the sacrificial ink lines are kept to shape the microgrooves (middle panel). c–f) The structural parameters of the microgrooves can be adjusted by controlling the printing parameters, such as c) the precuring time of the substrates, d) the concentration of the PAA inks, and e,f) the numbers of overlap printings. e) SEM sectional views of microgrooves fabricated with different printing layers.

great homogeneity of the networks over large areas. Scanning electron microscope (SEM) images of the networks are demonstrated in insets of Figure S10a, c (Supporting Information), suggesting that the microgrooves are interconnected at the crossing points. The microgrooves are labeled with fluorescent materials, as shown in Figure S10b, d (Supporting Information), which further manifests the interpenetrating networks of the printed microgrooves. The crossing microgrooves are of importance in microfluidic systems to construct devices such as microreactors.[28]

2.5. Patterning Mammalian Cells in the Microwells

The IIP-fabricated microwells and microgrooves could be widely utilized in biochips, microfluidics, functional devices, and other related fields.[29] Here, two demonstrations were given which regarding patterning various functional and biological materials in microwells and microgrooves. First, we demonstrated that fluorescent aqueous solution and mammalian cells could be trapped in the microwells. As shown in **Figure 4**a, microwell-matrix letter patterns were fabricated to demonstrate the flexibility of the printed features. Moreover, concave microwell–patterned PDMS surfaces showed large wettability contrast between the wells and the blank surfaces. Fluorescent aqueous solutions could be filled in the microwells to form fluorescent dot array (Figure 4b). The fluorescent intensity of the array indicated that the labeling of the microwells was homogeneous (Figure 4c). Additionally, the turnability of microwell size at the micrometer scale could be used to engineer biochips to construct cell patterns.[20b] Because a mammalian cell possessed a picoliter volume which was in

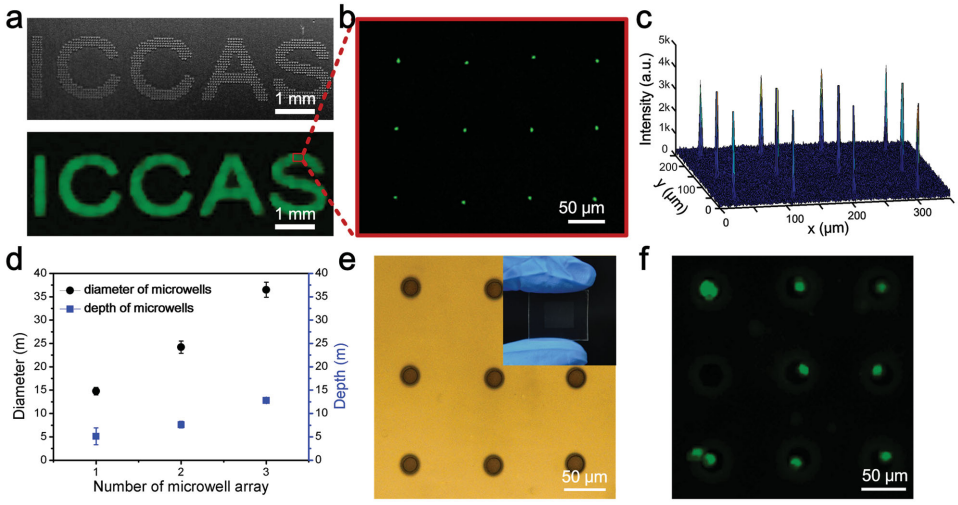

Figure 4. IIP-fabricated concave microwells with controllable sizes used to pattern fluorescent aqueous solutions and mammalian cells. a) Optical and fluorescent image of the microwell-matrix letter patterned PDMS surface after fluorescent labeling. b) Magnified confocal image of the fluorescent solution–filled microwell matrix. c) Fluorescent intensity of the matrix shown in (b), indicating the high homogeneity of the labeling. d) Three microwell arrays with different microwell sizes are fabricated to trap cells. The size parameters of the microwells are shown in the graph. e,f) Single cells can be trapped in the size-matched microwells to form single cell array. e) Optical image of a microwell array with diameter of 24.2 μm and depth of 7.6 μm. Inset is photograph of the microwell array printed on a transparent PDMS/PET substrate. f) Fluorescent image of the single cell array trapped in microwells.

order of magnitude with the printed microwells, a single cell could be assumed to be trapped in one printed microwell with matching size.[20b,c] Breast carcinoma cell line (MCF7) was used as a model to demonstrate the feasibility of patterning single cells in the microwells. To facilitate observation of the trapped cells, transparent PET films were used as the supporting layers to construct PDMS/PET substrates, as illustrated in inset in Figure 4e. The size of the microwells were adjusted through a layerwise printing manner to achieve cell trapping (Figure S11, Supporting Information). Three kinds of microwell arrays with different size parameters were used as shown in Figure 4d and Figure S12 (Supporting Information). Single cell arrays were formed in microwells with diameter of 24.2 μm and depth of 7.6 μm, as illustrated in Figure 4e,f. Bright field observation clearly demonstrated that one cell was trapped in a microwell (Figure S13, Supporting Information). For microwell with diameter of 14.8 μm and depth of 5.1 μm, cells could not be trapped, since the size of the microwell was too small for a cell (Figure S14a,b, Supporting Information). When the size of the microwells was increased, with diameter of 36.5 μm and depth of 12.8 μm, more than one cell was trapped in a microwell (Figure S14c, d, Supporting Information). Therefore, single cell array could be obtained with the assistance of size-matched microwells, which was of significance in single cell analyses.[20a]

2.6. Patterning Functional Materials in the Microgrooves

Patterning of functional materials in a defined position had tremendous potential for applications in integrated circuits, optoelectronics, magnetic devices, and microelectromechanical systems.[30] As a demonstration for the vigorous material patterning capability of the IIP-fabricated microgrooves, a wide range of functional nanoparticles including monodispersed polystyrene nanoparticles (PS NPs), cadmium selenide quantum dots (CdSe QDs), ferroferric oxide nanoparticles (Fe_3O_4 NPs), and silver nanoparticles (Ag NPs) were filled into the microgrooves and their networks, as shown in **Figure 5** and Figures S15–S18 (Supporting Information). The filled PS NPs assembled into photonic crystal microlines, endowing the microgrooves with vivid structural color, as shown in Figure 5a. SEM images in Figure 5b and Figure S15e (Supporting Information) showed that the PS NPs assembled into closely packed hexagonal structure, which has been achieved on flat surfaces and other confined structures.[31] The photonic crystal microline filled microgrooves would find various applications in microfluidic detections. Besides PS NPs, CdSe QDs were filled into the microgrooves and their networks, as demonstrated in Figure 5c,d and Figure S16 (Supporting Information). The CdSe QDs reserved fluorescent characteristics after patterning, resulted in a fluorescent network on the PDMS surface. The filling of Fe_3O_4 NPs was also conducted with immersing the microgrooves into Fe_3O_4 NP suspensions and subsequently pulled out. Optical and SEM images indicated that the filling was homogeneous in large area and the Fe_3O_4 NPs showed large distribution contrast in the microgrooves and on the surfaces (Figure S17, Supporting Information). Furthermore, conductive Ag NPs could be filled into the microgrooves and subsequently transfer-printed onto other substrates such as flexible PET surfaces to fabricate transparent conductive films.[32] The patterning and transferring process are illustrated in Figure 5e. Images of the Ag microwires before and after transferring are shown in Figure 5f, g. The transfer printing was conducted at 200 °C, which could on one hand soften the PET film to tailor the interfacial adhesion hence facilitate the transferring,[29c] and on the other hand sinter the Ag NPs to increase their conductance. As shown by the amplified image of a single transferred Ag microwire inserted in Figure 5g, the annealed Ag

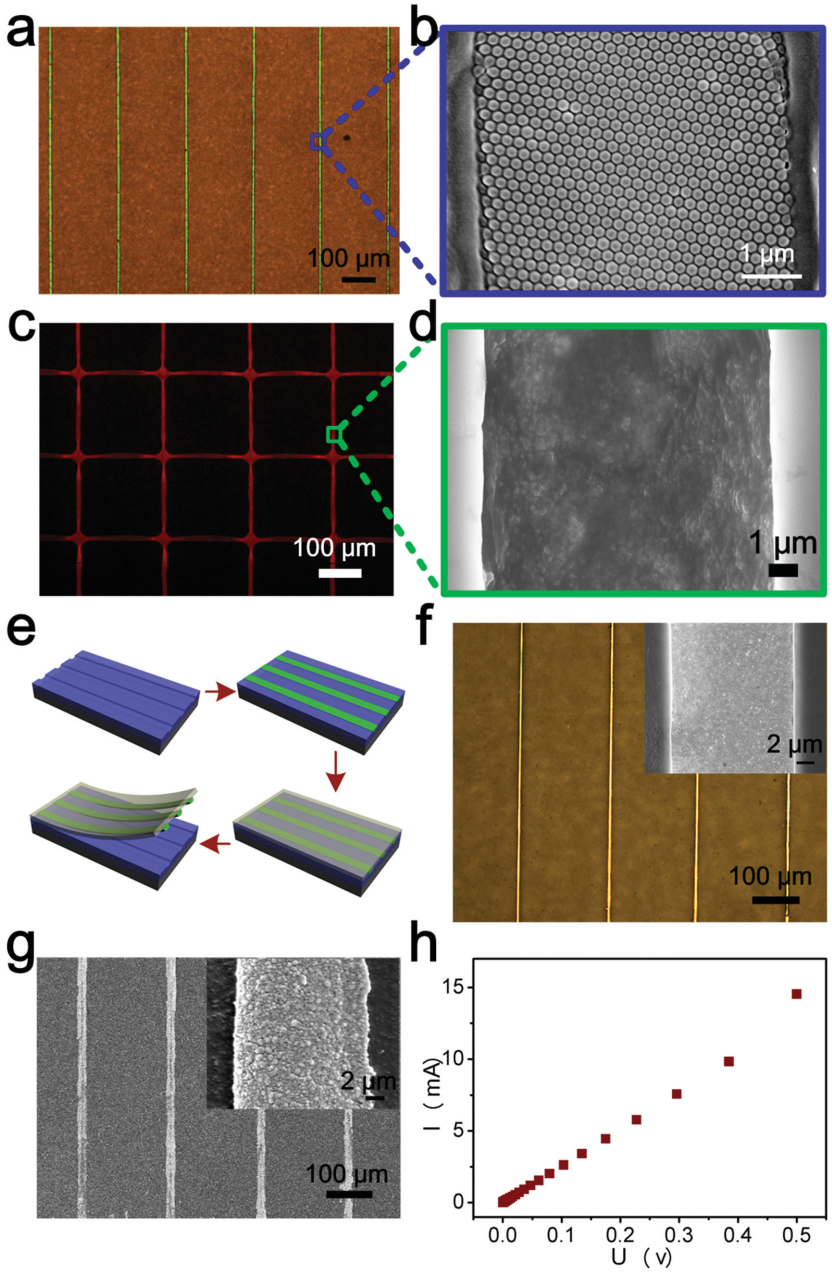

Figure 5. IIP-fabricated microgrooves used to pattern various functional nanoparticles and transfer print Ag NPs. a, b) PS NPs can be filled and assembled in the microgrooves. a) Optical image of the PS NP-filled microgroove array. b) SEM image of a single microgroove filled with PS NPs that are well assembled. c, d) CdSe QDs are patterned in the microgroove networks. c) Fluorescent images of the CdSe QD-filled microgroove network. d) SEM image of a single CdSe QD-filled microgroove. e–h) Ag NPs are patterned into the microgrooves and subsequently transfer-printed onto PET surfaces. e) Schematics of the patterning and transferring process. f) Optical image of the Ag NP-filled microgroove array. Inset is SEM image of a single microgroove filled with Ag NPs. g) SEM image of the Ag NP microwires transfer-printed onto PET surface. Inset is amplified image of a single silver microwire. h) Conducting characterization of the Ag NP microwires.

NPs possessed larger gain size, leading to a higher conductivity. The electrical resistivity of the printed Ag microwires was calculated by the current–voltage curve shown in Figure 5h and the sectional profile of the microwires shown in Figure S18 (Supporting Information). The resistivity of the Ag microwires reached 4.84×10^{-7} Ω m by annealing at 200 °C for 2 h. Moreover, the transparency of the Ag NP printed PET films was 91.6%, comparable to that of ITO (Figure S18, Supporting Information).[32]

3. Conclusions

In summary, a general IIP strategy was demonstrated to fabricate concave microstructures. By adjusting the interactions between the ink and the viscoelastic surfaces, the structural parameters of the microwells and microgrooves could be well controlled. The viscoelastic state of the printing substrates was of vital importance for controlling the concave microstructures. In addition, various functional materials including optical, electronic, and magnetic nanoparticles and mammalian cells could be patterned in the concave microstructures. This IIP technique will open a pathway to fabricate concave structures for patterning various materials. The resolution of a few micrometers of the microwells and microgrooves in this work could be further improved by increasing the dewetting of the inks,[7c] downscaling the diameter of the printing nozzles and using advanced printing methods. For example, the feature sizes of the microstructures could be further decreased down to submicrometer and even nanometer scales by taking advantage of the electrohydrodynamic jet printing.[33] Although the present materials used are a combination of viscoelastic PDMS precursor and water-based polymer solutions, the principle behind this methodology would make it possible to extend to a large number of material combinations, for instance, the combination of precured hydrogel substrates and oil-based inks, which would make the IIP a more general technique to fabricate various concave micro- or even nano-structures and functional devices.

4. Experimental Section

Preparation of Viscoelastic PDMS Surfaces: Alumina substrates (NanoThink Corp., China) and commercially available PET film cut into dimensions of approximately 3 × 3 cm and washed by deionized water and acetone for several times and dried in air, were used as supporting layers. PDMS (Sylgard 184, Dow Corning) base was mixed with a curing agent in the proportion of 10:1 by weight to make PDMS precursor. The precursor was put into a centrifuge to remove air

bubbles (7000 rpm, 5 min), then spin-coated onto the supporting layers (800 rpm for 10 s, then 3000 rpm for 30 s). Subsequently, the PDMS precursor was precured at 80 °C for 14–36 min and used as the printing substrate.

Fabrication of Concave Microstructures by IIP: PAA (M_w = 1800, Sigma-Aldrich, USA) dissolved in water/ethanol mixed solvent (with volume ratio 20:80) was used as the printing ink. The concentration of the ink ranged from 4 wt% to 20 wt%. The printing of the PAA ink was performed by a Dimatix Fujifilm DMP-2831 printer. Only one nozzle was used during the printing. The printing frequency was set at 3.0 kHz and a customized waveform was used, which had a maximum voltage of 40 V and a pulse width of 8.5 μs. Subsequently, the printed viscoelastic surfaces were heated at 80 °C for another 1 h to completely solidify the PDMS precursor. After washing with water for several times, microwell or microgroove arrays were left on the surfaces.

Trapping Cells in the IIP-Fabricated Microwells: Microwell-patterned PDMS/PET surfaces were placed in a culture dish. MCF7 cells in Dulbecco's modified eagle medium (DMEM) (1 mL) with a density of 1×10^6 mL^{-1} were applied onto the surfaces, then settled at 37 °C for 45 min. The cells not trapped in the microwells were removed by gentle washing with phosphate buffer saline (PBS) for several times. The trapped cells were stained with acridine orange (AO), in order to obtain fluorescent and bright filed images.

Patterning NPs in the IIP-Fabricated Microgrooves: Water-based suspensions of PS NPs (synthesized according to ref. [31]), CdSe QDs (purchased from Wuhan Jiayuan Quantum Dots Co. Ltd., China), Fe_3O_4 NPs (purchased from Beijing Sunrise Ferrofluid Technological Co. Ltd., China), and Ag NPs (synthesized according to ref. [32]) were prepared with solid contents ranging from 0.5 wt% to 5 wt%. Microgroove-patterned PDMS surfaces were immersed into the suspensions and subsequently pulled out slowly. After solvent evaporation, nanoparticles were filled into the microgrooves because of the capillary force and the hydrophobicity of the PDMS surfaces.

Instruments and Characterization: The structures and morphologies of the alumina surfaces, solid PDMS surfaces, and concave microstructure–patterned PDMS surfaces were investigated by an atomic force microscope (NSK SPA400, Japan), a field-emission scanning electron microscope (JSM-7500, Japan), and an optical microscope (Olympus MX40, Japan). The images showing the microwell-matrix letter patterns on the PDMS surfaces were taken by a digital camera (Canon 60D, Japan). The fluorescence image of the microwell matrix text patterns was taken by a fluorescence scanner (ChampChemi Professional+, China) in channel 535 nm with 365 nm UV light excitation. The height profiles of the microdots, microwells, and Ag microwires were determined in a surface profiler (Kosaka ET4000, Japan). FTIR characterization of the PDMS precursor surfaces was carried out on an infrared spectrometer (TENSOR 37, Germany). For the test potassium bromide pellet was used as the substrate and the spin-coating condition of PDMS precursor was kept the same as that of alumina surface. The nanoindentation test was carried out on a nanoindenter (HYSIRON TI 950, USA). The confocal fluorescence images were obtained using a laser confocal microscope (Olympus FV1000-IX81, Japan) with an excitation wavelength of 488 nm. The resistance of the transferred Ag microwire was measured with a Keithley 4200-SCS semiconductor analyzer.

Supporting Information

Supporting Information is available from the Wiley Online Library or from the author.

Acknowledgements

This work was supported by the 973 Program (2013CB933004), the NSFC (Grant Nos. 51173190 and 21121001), and the "Strategic Priority Research Program" of the Chinese Academy of Sciences (Grant No. XDA09020000). The authors declare no competing financial interests. Dr. Lang Jiang from Cavendish Laboratory, University of Cambridge is acknowledged for the helpful suggestions.

Received: March 6, 2015
Revised: April 7, 2015
Published online: April 27, 2015

[1] A. L. Briseno, S. C. B. Mannsfeld, M. M. Ling, S. H. Liu, R. J. Tseng, C. Reese, M. E. Roberts, Y. Yang, F. Wudl, Z. N. Bao, *Nature* **2006**, *444*, 913.
[2] a) M. Trupke, J. Goldwin, B. Darquie, G. Dutier, S. Eriksson, J. Ashmore, E. A. Hinds, *Phys. Rev. Lett.* **2007**, *99*, 4; b) R. P. Camare, A. Best, S. K. Nett, J. S. Gutmann, E. Bonaccurso, *Opt. Express* **2007**, *15*, 9877.
[3] J. Ziauddin, D. M. Sabatini, *Nature* **2001**, *411*, 107.
[4] R. Osellame, H. Hoekstra, G. Cerullo, M. Pollnau, *Laser Photon. Rev.* **2011**, *5*, 442.
[5] A. Carlson, A. M. Bowen, Y. Huang, R. G. Nuzzo, J. A. Rogers, *Adv. Mater.* **2012**, *24*, 5284.
[6] A. H. O. Karkkainen, J. T. Rantala, A. Maaninen, G. E. Jabbour, M. R. Descour, *Adv. Mater.* **2002**, *14*, 535.
[7] a) E. Tekin, P. J. Smith, U. S. Schubert, *Soft Matter* **2008**, *4*, 703; b) B. Derby, *Annu. Rev. Mater. Res.* **2010**, *40*, 395; c) M. Kuang, L. Wang, Y. Song, *Adv. Mater.* **2014**, *26*, 6950; d) M. Singh, H. M. Haverinen, P. Dhagat, G. E. Jabbour, *Adv. Mater.* **2010**, *22*, 673.
[8] S. B. Walker, J. A. Lewis, *J. Am. Chem. Soc.* **2012**, *134*, 1419.
[9] H. Sirringhaus, T. Kawase, R. H. Friend, T. Shimoda, M. Inbasekaran, W. Wu, E. P. Woo, *Science* **2000**, *290*, 2123.
[10] A. Teichler, R. Eckardt, S. Hoeppener, C. Friebe, J. Perelaer, A. Senes, M. Morana, C. J. Brabec, U. S. Schubert, *Adv. Energy Mater.* **2011**, *1*, 105.
[11] H. M. Haverinen, R. A. Myllyla, G. E. Jabbour, *J. Disp. Technol.* **2010**, *6*, 87.
[12] K. Crowley, E. O'Malley, A. Morrin, M. R. Smyth, A. J. Killard, *Analyst* **2008**, *133*, 391.
[13] B. Derby, *Science* **2012**, *338*, 921.
[14] a) T. Kawase, H. Sirringhaus, R. H. Friend, T. Shimoda, *Adv. Mater.* **2001**, *13*, 1601; b) B. J. de Gans, S. Hoeppener, U. S. Schubert, *Adv. Mater.* **2006**, *18*, 910; c) D. Kwak, J. A. Lim, B. Kang, W. H. Lee, K. Cho, *Adv. Funct. Mater.* **2013**, *23*, 2524.
[15] X. H. Zhang, X. X. Wei, W. Ducker, *Langmuir* **2010**, *26*, 4776.
[16] a) S. Y. Chou, P. R. Krauss, P. J. Renstrom, *Appl. Phys. Lett.* **1995**, *67*, 3114; b) L. J. Guo, *Adv. Mater.* **2007**, *19*, 495; c) H. J. Park, M. G. Kang, L. J. Guo, *ACS Nano* **2009**, *3*, 2601.
[17] T. H. J. van Osch, J. Perelaer, A. W. M. de Laat, U. S. Schubert, *Adv. Mater.* **2008**, *20*, 343.
[18] a) A. Carre, J. C. Gastel, M. E. R. Shanahan, *Nature* **1996**, *379*, 432; b) M. E. R. Shanahan, A. Carre, *Langmuir* **1995**, *11*, 1396; c) A. Alizadeh, V. Bahadur, W. Shang, Y. Zhu, D. Buckley, A. Dhinojwala, M. Sohal, *Langmuir* **2013**, *29*, 4520.
[19] a) S. J. Park, B. M. Weon, J. S. Lee, J. Lee, J. Kim, J. H. Je, *Nat. Commun.* **2014**, *5*, 4369; b) R. Pericet-Camara, G. K. Auernhammer, K. Koynov, S. Lorenzoni, R. Raiteri, E. Bonaccurso, *Soft Matter* **2009**, *5*, 3611.
[20] a) S. Lindstrom, H. Andersson-Svahn, *Lab Chip* **2010**, *10*, 3363; b) J. R. Rettig, A. Folch, *Anal. Chem.* **2005**, *77*, 5628; c) J. Jin, Y. Z. Xing, Y. L. Xi, X. L. Liu, T. Zhou, X. X. Ma, Z. Q. Yang, S. T. Wang, D. S. Liu, *Adv. Mater.* **2013**, *25*, 4714.
[21] Y. L. Wang, H. H. Lai, M. Bachman, C. E. Sims, G. P. Li, N. L. Allbritton, *Anal. Chem.* **2005**, *77*, 7539.
[22] H. Zhao, K. Y. Law, *Langmuir* **2012**, *28*, 11821.

[23] H. Park, H. Cho, J. Kim, J. W. Bang, S. Seo, Y. Rahmawan, D. Y. Lee, K. Y. Suh, *Small* **2014**, *10*, 52.
[24] D. Soltman, V. Subramanian, *Langmuir* **2008**, *24*, 2224.
[25] P. C. Duineveld, *J. Fluid Mech.* **2003**, *477*, 175.
[26] B. J. de Gans, P. C. Duineveld, U. S. Schubert, *Adv. Mater.* **2004**, *16*, 203.
[27] B. Y. Ahn, E. B. Duoss, M. J. Motala, X. Y. Guo, S. I. Park, Y. J. Xiong, J. Yoon, R. G. Nuzzo, J. A. Rogers, J. A. Lewis, *Science* **2009**, *323*, 1590.
[28] C. K. Chung, T. R. Shih, C. K. Chang, C. W. Lai, B. H. Wu, *Chem. Eng. J.* **2011**, *168*, 790.
[29] a) T. L. Downing, J. Soto, C. Morez, T. Houssin, A. Fritz, F. L. Yuan, J. L. Chu, S. Patel, D. V. Schaffer, S. Li, *Nat. Mater.* **2013**, *12*, 1154; b) R. Seemann, M. Brinkmann, E. J. Kramer, F. F. Lange, R. Lipowsky, *Proc. Natl. Acad. Sci. U. S. A.* **2005**, *102*, 1848; c) T. Kraus, L. Malaquin, H. Schmid, W. Riess, N. D. Spencer, H. Wolf, *Nat. Nanotechnol.* **2007**, *2*, 570.
[30] a) Z. H. Nie, E. Kumacheva, *Nat. Mater.* **2008**, *7*, 277; b) E. Menard, M. A. Meitl, Y. G. Sun, J. U. Park, D. J. L. Shir, Y. S. Nam, S. Jeon, J. A. Rogers, *Chem. Rev.* **2007**, *107*, 1117.
[31] Y. Huang, J. M. Zhou, B. Su, L. Shi, J. X. Wang, S. R. Chen, L. B. Wang, J. Zi, Y. L. Song, L. Jiang, *J. Am. Chem. Soc.* **2012**, *134*, 17053.
[32] Z. L. Zhang, X. Y. Zhang, Z. Q. Xin, M. M. Deng, Y. Q. Wen, Y. L. Song, *Adv. Mater.* **2013**, *25*, 6714.
[33] J. U. Park, M. Hardy, S. J. Kang, K. Barton, K. Adair, D. K. Mukhopadhyay, C. Y. Lee, M. S. Strano, A. G. Alleyne, J. G. Georgiadis, P. M. Ferreira, J. A. Rogers, *Nat. Mater.* **2007**, *6*, 782.